Foundation load analysis of Oyster® using a five degree of freedom load transducer

Damien Howard[1], Trevor Whittaker[1,2] and Kenneth Doherty[2]

[1]Wave Energy Research Group, School of Planning Architecture and Civil Engineering, Queen's University Belfast, Belfast BT9 5AG, UK

[2]Aquamarine Power Limited, 10 Saint Andrew Square, Edinburgh, EH2AF, UK

Abstract

The Oyster® Oscillating Wave Surge Converter is a seabed mounted wave energy device that consists of a buoyant flap that is free to oscillate about a pivot. It completely penetrates the water column and is located within the near shore region in a water depth of 13m.

As with any marine wave energy converter the foundation design and the survivability characteristics of the device itself are of paramount importance.

To address this issue an extensive series of experiments was carried out to investigate the foundation loads experienced by the device in extreme sea conditions. Experiments were conducted using a scale model of Oyster® and the resultant foundation loads were measured using a five degree of freedom load transducer developed specifically for this purpose.

This paper will discuss the design, calibration and operation of the five degree of freedom load transducer as a well as a discussion on error checking procedures used to verify the accuracy and resolution of the device.

Samples of the data generated during the test series are presented to demonstrate the operation of the load transducer. A discussion of Extreme Value Analysis (EVA) data processing techniques used to estimate the loading upon the flap for a range of events with increasing return periods is also presented.

Keywords: extreme loading, extreme value analysis, load transducer design and operation, tank testing.

Nomenclature

K	=	calibration matrix
F	=	force matrix
V	=	signal output matrix
Hs	=	significant wave height
Te	=	energy period
Q_1	=	first quartile
Q_3	=	third quartile
IQR	=	inter quartile range
P	=	probability of non-exceedance
m	=	data rank
N	=	total number of elements
R	=	return period

1. Introduction

Oyster® consists of a buoyant flap that oscillates about a pivot that is mounted to the sea floor at a water depth of approximately 13 metres. Cylinders connected to the flap convert the oscillatory motion to hydraulic pressure which pumps freshwater through a high pressure pipeline to shore.

The water within the pipe is then expelled through a valve onto a Pelton wheel connected to a generator, which produces electrical power. The system is presented graphically in Fig. 1. Refer to [1-2] for a more detailed discussion of the operation and design of Oyster®.

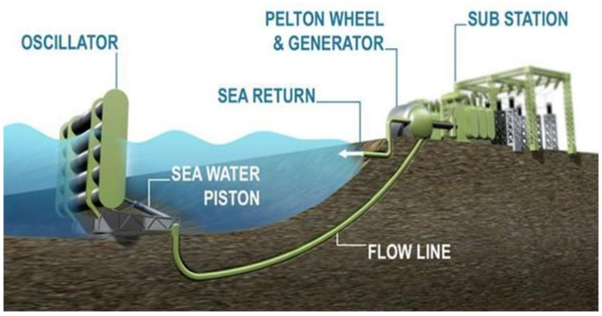

Figure 1: Operation of Oyster®

By placing Oyster® in the shallow water environment the device is sheltered from extreme loading during storm conditions since most large waves will break before reaching it due to shoaling effects. As the magnitude of the waves incident upon Oyster® increase, the device progressively decouples from the waves thus providing a natural safety mechanism to minimise the foundation loads experienced by the device.

Despite the ability of Oyster® to decouple from the most extreme waves, it is inevitable that extreme loading events will occur and in order to address these concerns, a series of experiments were conducted to measure the loads experienced by Oyster® under extreme sea conditions.

The extreme sea states used in the test series were derived from the hindcast data from the proposed Oyster® installation site at the European Marine Energy Centre (EMEC).

The set of sea states used provides a range of wave breaking scenarios which explore the effect wave breaking type and location have upon the foundation loads.

In order to facilitate these investigations research into the design and implementation of novel five degrees of freedom (DoF) load transducer was undertaken that led to the development of the device outlined in this paper.

2. Transducer design

The basic design and operating principle of the five DoF elbow transducer is based on that proposed in [3], which consists of a strain gauged tubular structure with end flanges. While this transducer design is capable of resolving shear loads and moments perpendicular to the major axis of the device it is unable to provide any reasonable measurements of loads applied along this axis due to the axial stiffness of the transducer. This limitation can be overcome by incorporating a strain gauged cantilevered platform underneath the tubular section of the transducer. This provides the required resolution in that DoF which gives meaningful results as outlined in [4].

The five DoF device outlined in this paper differs from the concept proposed by [4] in that instead of using a cantilevered platform to resolve axially applied loads, it incorporates a second tubular component orientated perpendicular to the first and is presented schematically in Fig. 2.

3. Strain gauging

Each cylindrical section of the transducer has three full Wheatstone bridges attached along its length. Two of the bridges are placed at one end of the cylinder, each bridge consisting of two strain gauge pairs.

The location of the four strain gauge pairs denoted by S1, S2, S3 and S4 in Fig. 2 are aligned parallel to the main axis of the cylinders with each capable of measuring bending moments about two orthogonal planes.

Torsion about the axial plane of each cylinder is measured using 90^0 rosette gauges that are orientated at 45^0 to the axis of the cylinder. These are placed at the other end of the tubular section relative to the other gauges and are labelled S3 and S6 as shown in Fig. 2.

Strain gauges with a resistance of 125 ohms and an operation voltage of 6V were selected and the outputs from these are passed through an amplifier with a gain of 800 applied to each signal. Following strain gauging each cylinder is waterproofed along its length using rubber sealant.

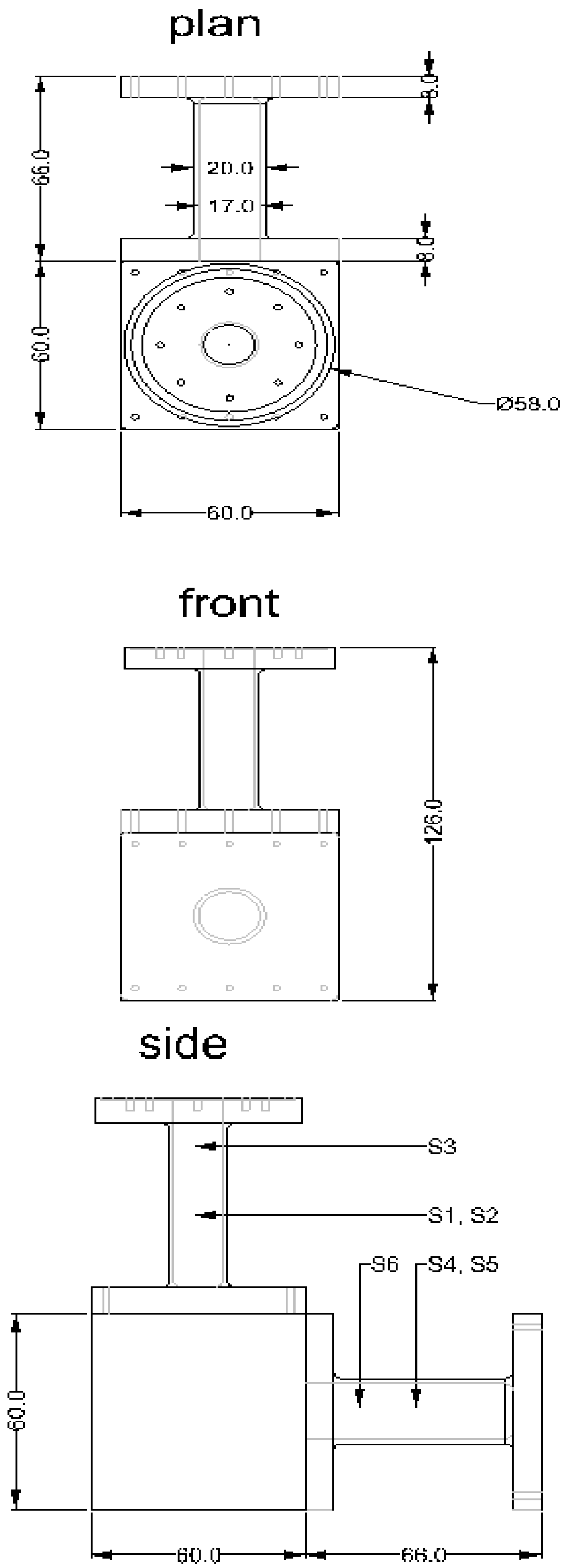

Figure 2: Schematic diagram of five degree of freedom load transducer and strain gauge position (units in mm)

4. Calibration

Before the load transducer can be used in wave tank experiments it must first be calibrated so that the electrical signal outputs from S1 to S6 (mV) is converted into units of Newtons (N) and Newton metres (Nm).

The calibration of the load transducer has been carried out using the linear approach as outlined in [5-6], where each signal output from the load transducer is expressed as a linear combination of the components of the applied loads. Given in Fig. 3 is an idealised representation of the transducer showing the location of each gauge. Also given is the sign convention used for six degrees of freedom.

Given in **Equations 1** to **6** is the idealised relationship of each strain gauge (S1 to S6) to loads applied in each DoF were **a**, **b** and **c** are moment arm lengths as defined in Fig. 3.

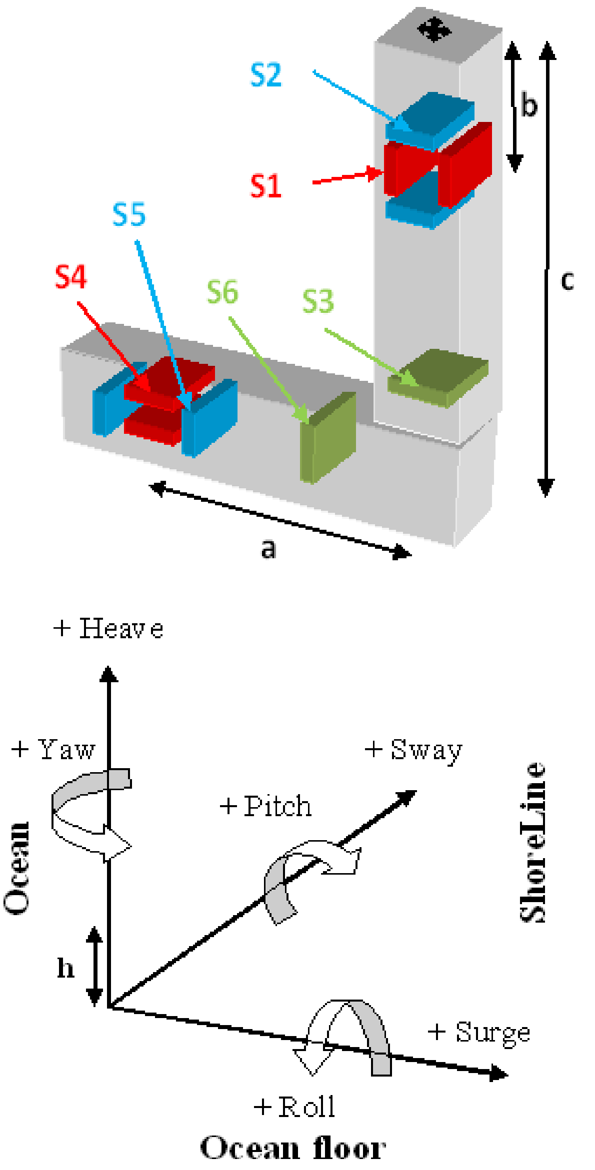

Figure 3: Location of strain gauges and load sign convention

Writing out the equations in this form shows explicitly the need for the external measurement of pitch and highlights the hierarchical relationship between the strain gauge outputs when attempting to resolve the loads.

$$S_1 = (b \times Surge) + Pitch \qquad \text{(Eq.1)}$$

$$S_2 = (b \times Sway) - Roll \qquad \text{(Eq.2)}$$

$$S_3 = Yaw \qquad \text{(Eq.3)}$$

$$S_4 = (a \times Heave) + (c \times Surge) + Pitch \qquad \text{(Eq.4)}$$

$$S_5 = (a \times Sway) + Yaw \qquad \text{(Eq.5)}$$

$$S_6 = (c \times Sway) - Roll \qquad \text{(Eq.6)}$$

With the inclusion of the pitch moment, the system is over-defined and the remaining five DoF become resolvable. This pitch moment, with units of Nm, is measured using separate torque transducers that are attached to the flap and measure the applied damping that is placed on the flap by Coulomb friction brakes used to simulate the power take off system.

Since the strain gauges are attached to the same body all strain gauges are mechanically coupled to one another and thus there is crosstalk between each gauge. This crosstalk means that the voltage-load relationship deviates from that outlined in **Equations 1** to **6** and must be accounted for.

Compensation for this crosstalk is accomplished by deriving a calibration matrix **K** that relates the response of individual channels when a single load is applied to the system as shown in **Equation 7**, with components of each written out explicitly in **Equation 8**.

$$F = KV \qquad \text{(Eq. 7)}$$

$$\begin{pmatrix} Heave \\ Surge \\ Sway \\ Roll \\ Yaw \end{pmatrix} = \begin{pmatrix} k_{11} & \cdots & k_{17} \\ \vdots & \ddots & \vdots \\ k_{51} & \cdots & k_{57} \end{pmatrix} \begin{pmatrix} S1 \\ S2 \\ S3 \\ S4 \\ S5 \\ S6 \\ Pitch \end{pmatrix} \qquad \text{(Eq. 8)}$$

In order to determine the components of **K**, a series of combination loads is applied to the load transducer. A total of 203 load combinations, given in Table 1, were applied to the system with the outputs S1 to S6 being measured for each and the applied pitch calculated analytically (when applicable).

The outputs S1-S6 are then combined with the calculated pitch in order to create a 7x203 matrix, $\mathbf{V}_{\mathbf{Calib}}$. The corresponding applied loads are stored in a separate 5x203 load matrix, $\mathbf{F}_{\mathbf{Calib}}$.

The calibration matrix, **K**, which related the signal output and applied pitch to the actual loading applied to the system, can then be derived from a least-square best fit applied to the calibration data. Thus **K** is determined by:

$$K = F_{calib} V_{calib}^{T} \left(V_{calib} V_{calib}^{T} \right)^{-1} \quad \text{(Eq.9)}$$

Load combination	Number of data points
Heave and Roll	50
Heave and Pitch	42
Sway and Yaw	25
Sway and Roll	12
Surge and Yaw	50
Surge and Pitch	24

Table 1: Load combinations used during calibration

It is important to note that since the derivation of **K** relies upon the inclusion of an independent measurement of pitch from the torque transducers it is necessary to carry out the calibration along the axis about which the pitch moment acts. For the Oyster® device this is located at the pivot point about which the flap oscillates. This also has the added benefit that it resolves all loads acting on Oyster® to the plane of the pivot and thus provides a consistent reference point when designing/modifying the geometry of the device.

Given in **Equation 10** is the calibration matrix **K** calculated for the load transducer using the method outlined above:

$$\mathbf{K} = \begin{pmatrix} 352 & -32 & -29 & -239 & 18 & -50 & -6 \\ 221 & -55 & -49 & -3 & 33 & -86 & -12 \\ 4 & -153 & 222 & -0.7 & -147 & -235 & -0.1 \\ -0.3 & -25 & 25 & 0.2 & -16 & -10 & -0.006 \\ 0.1 & 12 & -18 & 0.2 & -7 & 18 & -0.1 \end{pmatrix} \quad \text{(Eq.10)}$$

In order to check the validity of the method used in deriving the above calibration matrix it is multiplied by $\mathbf{V_{Calib}}$. This results in the generation of the $\mathbf{F^1}$ matrix, the values of which having a standard deviation of less the 1% when compared with $\mathbf{F_{Calib}}$. Further calibration checks were carried out by applying an additional range of static loads to the transducer at the pivot point. From these calibration checks the error associated with each DoF are calculated to within 2% for the heave and surge and less than 1% in the remaining DoF.

In addition to the calibration checks outlined above a further series of tests were carried out in order to examine the effect on the calculated loads when an eccentric moment is applied to the load transducer. This was accomplished by applying a known pure static moment at various heights above the load transducer; in this case a pitch moment was applied at the top flange of the transducer, the pivot height and twice the pivot height above the transducer. A pitch moment was used in these tests as it is vital for the calculation of the remaining degrees of freedom of which heave and surge are of most importance. From these tests it was found that the eccentricity of the pitch moment has little effect upon the heave and surge loads measured by the transducer, the maximum error associated with heave and surge being 0.5N and 0.7N per Nm of applied pitch respectively.

5. Experimental tank testing

Since the survivability of any wave power device is of paramount importance when considering possible design and mooring strategies, a comprehensive investigation was carried out in order to try and quantify the foundation loads that Oyster® is expected to encounter. All testing has been carried out in the wave tank at Queens University Belfast which utilises six sector-carrier wave makers capable of generating realistic sea-states.

The sea-states used were generated from 9 years of hindcast data from the European Marine Energy Centre (EMEC) site and were chosen to provide a representative sample of extreme seas.

Extreme seas are defined as sea-states with a significant wave height, Hs, greater than 6m. Given in Table 2 is a summary of the sea-states (defined using the Bretschneider spectrum) used to examine the foundation loads.

In order for a comprehensive and robust treatment of the foundation loads to be carried out it is desirable that the test run length used is a long as possible. This provides sufficient time for the generated sea states to “build up” and provide a higher probability that particular wave/flap interactions that could potentially lead to extreme loads will occur.

Sea State	*Energy Period Te (s)*	*Significant wave height Hs (m)*
1	9	10
2	11	10
3	13	8
4	13	10
5	15	8
6	15	10

Table 2: Extreme sea states used during testing

In order to maximise the chance of these wave/flap interactions occurring each of the test seas are run for 34 minutes and 8 seconds (2048 seconds). This equates to a full scale run time of 215 minutes (3 hours 35 minutes) per sea state and 1290 minutes (approx. 21 hours) over all six sea states tested. A sampling rate of 64Hz was used for the data acquisition.

From the hindcast data obtained for the EMEC site it was calculated that the average number of hours of extreme sea conditions per annum is approximately 26.9 hours, with more than half of these sea states having a significant wave height of less than 7m. Thus the experimental testing of 21 hours at larger sea conditions can be taken as a reasonable if not conservative estimate of the storm conditions the device may encounter during an average year.

It should also be noted that each extreme sea state used is given the same weighting factor. The full scale significant wave heights reported in Table 2 are the demand value wave heights which are slightly above what is achievable in the wave tank.

It is difficult to estimate the significant wave height of the waves at the model position due to effects introduced by wave breaking and the inability of wave probes to accurately measure the wave height in an aerated liquid. Thus the sea state values should only be taken as a estimate of the representative wave height at the model position.

The model position and bathymetry used in these tests is given in Fig. 4, the model being located in a full scale mean water depth of 13m.

The Oyster® device consists of a flap which has a full scale height (top of flap to pivot) of 10.6m and a thickness 1.8m. When the device is installed at the EMEC site it is envisaged that the pivot will be located 4m above the seabed, with the gap created between the bottom of the device and the seabed being completely filled.

The 40th scale model representation of Oyster® consists of a flap constructed using a PVC backbone with a foam covering, which is then mounted on two separate watertight instrumentation arrays (Fig. 5a). Each instrumentation array contains a rotary potentiometer, used to measure the angular rotation of the flap, a Coulomb friction brake, used to apply constant damping to the flap as well as a torque transducer used to measure the applied damping (Fig. 5b).

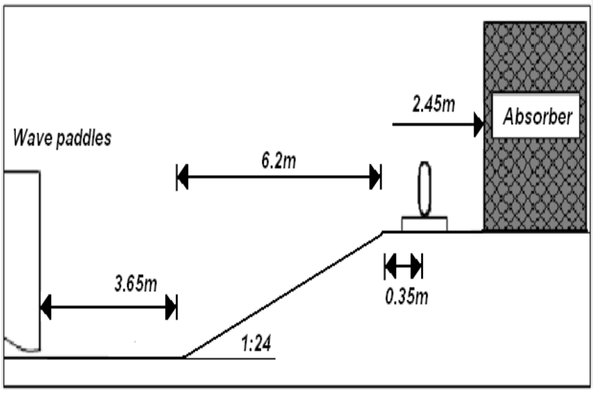

Figure 4: QUB wave tank setup (not to scale)

The instrumentation arrays are attached to a 12mm thick base plate which is then in turn fixed to the top flange of the load transducer (Fig. 5c). The load transducer is attached to an L bracket which is bolted to the tank floor.

Once the model is mounted upon the load transducer there is a 62mm gap between the bottom of the base plate and the tank floor. This gap is filled using a 60x60mm block of wood, which covers the gap sufficiently to prevent flow underneath the model while providing 2mm of clearance between the base plate and block to ensure that all loads are transferred directly through the transducer.

It is important to note that in this test configuration the vertical cylinder of the load transducer is protruding above the tank floor. Any wave load incident directly upon the vertical cylinder must be prevented since it could contaminate the results and thus a wooden block is placed in front of the transducer to prevent and loads being directly applied to the vertical cylinder.

During the investigation of the foundation loads two separate operating modes were considered; loading experienced with no applied damping placed on the flap and the loading with damping applied to the flap.

This was done in order to estimate the effect the applied damping has upon the loads and whether the device can safely generate power under extreme sea conditions.

For any sea state, a device will have an optimum damping torque where the power captured is maximized. However, during the extreme sea tests only one constant global damping value was applied for all six sea states. This global damping is determined from a weighted average of the optimal damping values, which was determined during independent tests using production seas.

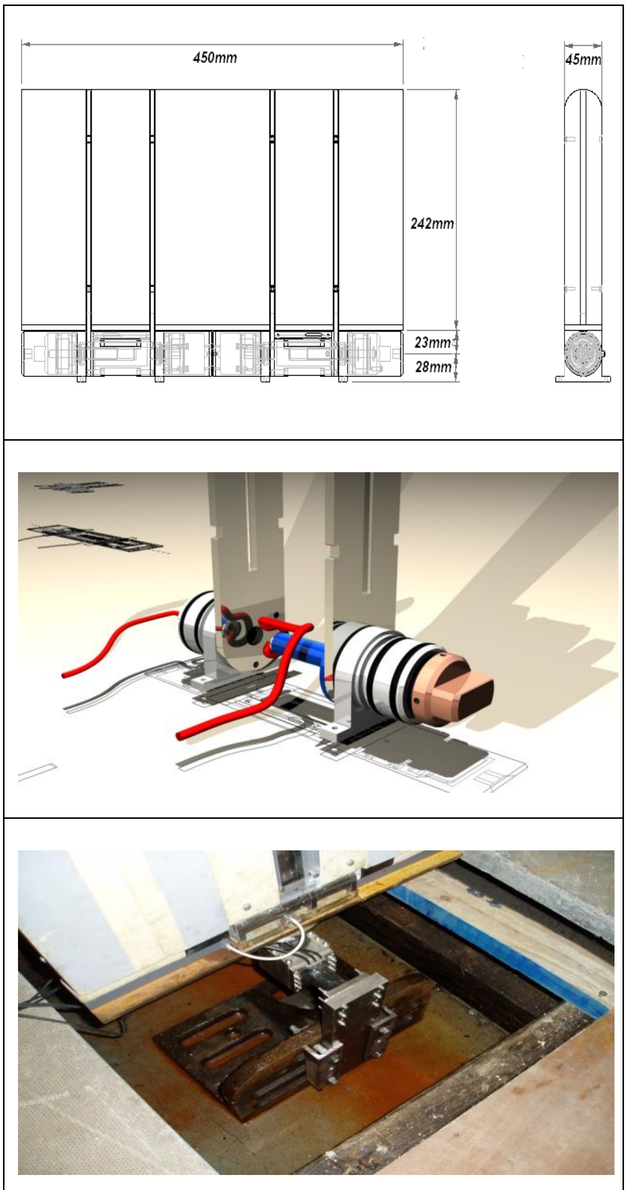

Figure 5: 40th scale model instrumentation and setup

6. Results

Presented in Figs. 6 and 7 are scatter plots that show the measured full scale heave and surge loads versus the angular rotation of the flap (from vertical) for both the damped and undamped case. Also presented in Figs. 6 and 7 is a typical loading curve created as the flap oscillates through one full cycle, the path followed by the loads denoted by arrows.

It can be clearly seen that the measured loads increased only slightly when damping is applied to the flap. This is also the case for the loading experienced in the other DoF as can be seen in Table 3 which shows the effect of applied damping upon foundation loads relative to the undamped loads.

This implies that even in extreme sea conditions the device will still be capable of safely generating power. It should be noted that since the pitch experienced by the device is equivalent to the applied constant damping placed on the flap it will always have the same value in all sea states and has thus been omitted from Table 3.

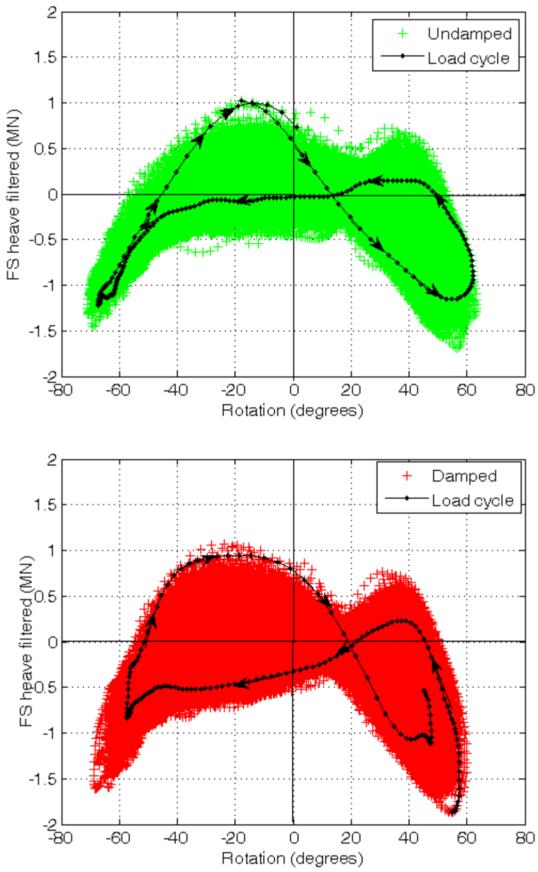

Figure 6: Sea state 3 Undamped and damped heave versus rotation scatter plot

Presented in Fig. 8 is scatter plot of coincident heave versus surge loads experienced by the damped device. From the coincident heave and surge loading data it was calculated that the peak resultant of these loads acts between -12^0 and -21^0 relative to the horizontal plane in the southeast quadrant, for all sea states.

The location and direction of the peak resultant implies that the contributing loads to this are positive surge and negative heave, the shallow angle relative to the horizontal plane indicating that the positive surge is the dominate factor.

Please note that while the peak resultant load vector gives the magnitude and direction of the largest heave/surge combination measured there may exist other resultant load combinations that are more important when considering the foundation design.

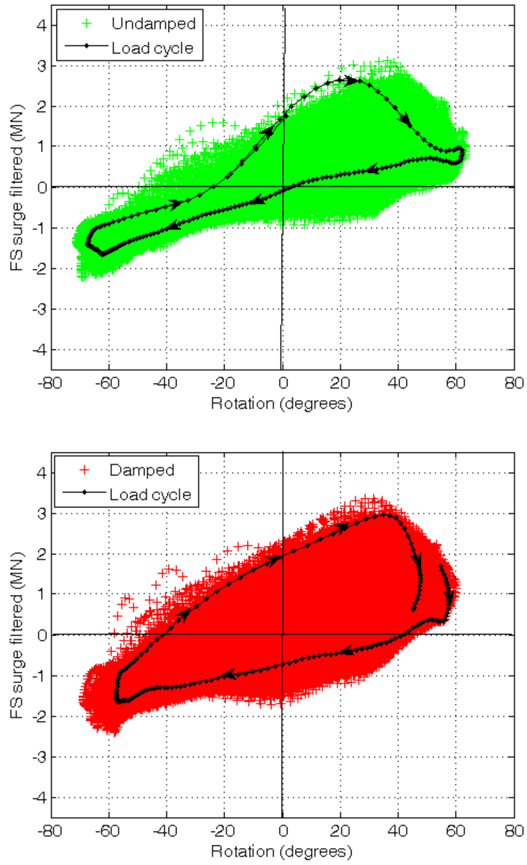

Figure 7: Sea state 3 Undamped and damped surge versus rotation scatter plot

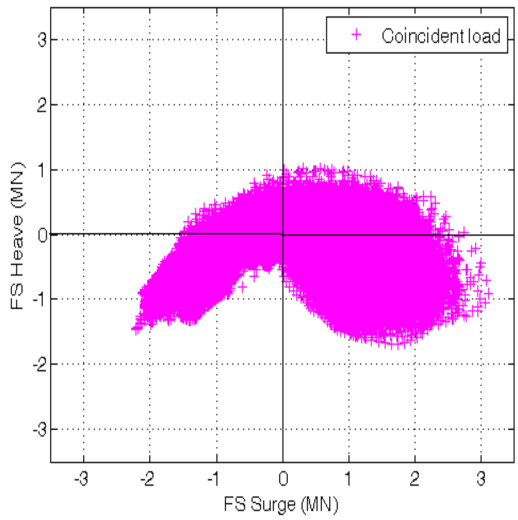

Figure 8: Sea state 3 Undamped coincident surge versus heave scatter plot

Load	damped:undamped positive load ratio	damped:undamped negative load ratio
Heave	0.77	1.09
Surge	1.11	1.02
Sway	1.08	1.3
Roll	1.01	1.07
Yaw	0.93	1.07

Table 3: Effect of applied damping upon foundation loads relative to undamped loads

Examining the scatter plots presented in Fig. 6 it can be seen that the heave load cycles experienced by the device have a very distinctive shape associated with them.

As will be shown in the following paragraphs the heave load experienced by the flap during a typical cycle can be expressed as a combination of flap buoyancy, vertical centrifugal force associated with the rotating flap and the interaction between the flap and the water particle motion in the wave. Video analysis was also used in conjunction with the recorded data to examine the load cycles.

At Point **A** in Figs. 9 and 10, the flap is submerged by the leading edge of an incoming wave and is rotating with a high velocity toward the beach. At this point the effects of flap buoyancy, the vertical component of the centrifugal force and the water particle motion combine to give a maximum heave event.

As the wave passes over the flap it pitches backward at a large angle of rotation denoted by **B**. At this point the water particle motion is acting downward on the flap which results in a negative heave.

At Point **C** the wave has nearly passed the flap, however the flap is still fully submerged. As a result the static buoyancy dominates and the flap experiences a positive heave force.

Between points **C** and **E**, the flap moves into the trough of the next incoming wave. The lower water level present in the wave trough reduces the buoyancy so that the flap "feels" more of its own weight and the heave load becomes negative. It can be seen that at **D** the vertical centrifugal force increases due to the flap rotating at a high velocity, however it cannot compensate completely for the reduction in buoyancy caused by the lower water level.

Between points **E** and **F** the flap enters the incoming wave and thus the effects of water particle motion, vertical centrifugal force and static buoyancy combine again to increase the heave load and complete the cycle.

It is important to note that while the three main contributors to the heave load cycle are the flap buoyancy, the vertical centrifugal force and the local water particle motion, the contribution each makes to the total heave load will vary from wave to wave. This is due to variations in the characteristics of the incident wave as well as the orientation of the flap when it encounters the wave.

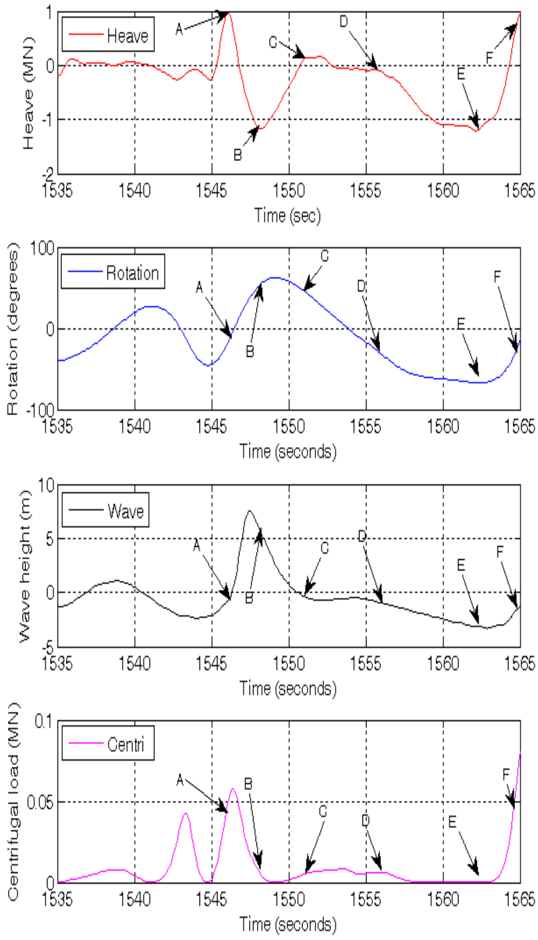

Figure 9: Heave load, flap rotation, wave height and vertical centrifugal force for one heave load cycle

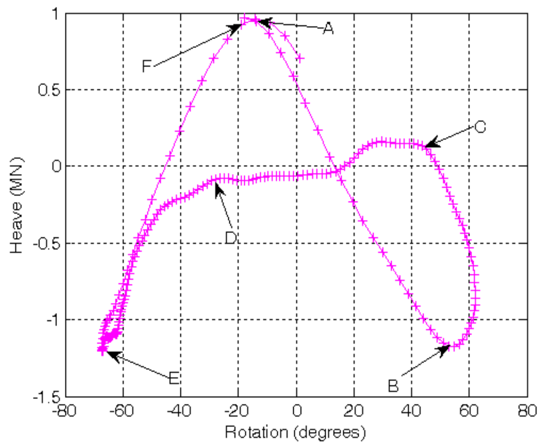

Figure 10: Heave versus rotation load cycle

Presented in Figs. 11 and 12 are box plots of the full scale heave and surge load measured during the extreme sea tests for the globally damped case. For each sea state the foundation loads are split up into positive and negative sets and the peaks in the data are found and arranged in ascending order of magnitude.

The median of the data set is calculated, represented by the horizontal red line, and about this a box is drawn which is bounded by the first and third quartiles, Q_1 and

Q_3, which indicate the 25 and 75 percentile levels respectively. The vertical black lines which terminate with an 'o' symbol, define the range outside of which the data points are considered outliers. This range extends from Q_1 - 1.5(IQR) to Q_3 + 1.5(IQR) where IQR the Inter-Quartile Range is defined as the 'distance' between the first and third quartiles and can be given by IQR=$|Q_3 - Q_1|$.

The maximum and minimum outliers for each foundation load in each sea state are denoted with a green asterex. The box plots give an indication of the distribution of the peak foundation loads and also show the scatter of extreme loading events represented by the asterex.

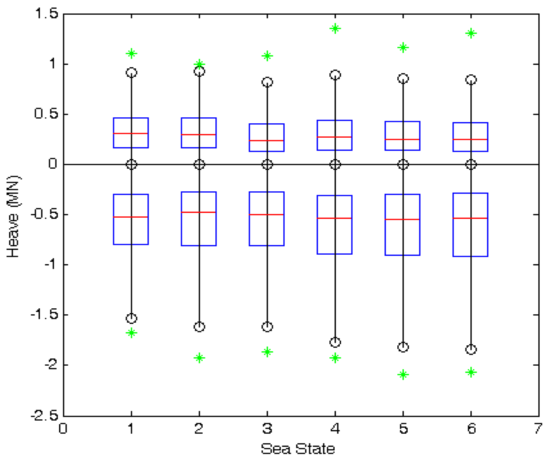

Figure 11: Heave load for globally damped 18m wide, 1.8m thick damped flap in each extreme sea state

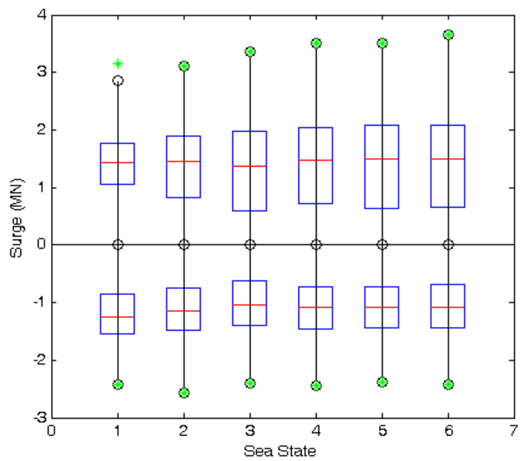

Figure 12: Surge load for globally damped 18m wide, 1.8m thick damped flap in each extreme sea state

7. Extreme Value Analysis

While selecting the largest extreme event out of the six sea states tested will provide an estimate of the typical load the device must withstand. It is important to note that due to the finite run length used during the test series, *there is no guarantee that during this period the combination of conditions that result in maximum loads have occurred*.

In order to address these concerns an extreme value analysis of the data is required to determine the peak loads that the device may encounter during its operational lifetime.

Extreme value analysis as outlined in [7] is based on the extrapolation of the cumulative distribution function, CDF, which is based on the probability that an extreme load will not be exceeded in one time step. To produce the CDF, the loading data for each DoF is split into positive and negative sets and the peak events found. The peaks from all sea states are combined and are then ranked in ascending order of magnitude. The probability of non-exceedance, **P**, is given by:

$$P = \frac{m}{N+1} \qquad \text{(Eq.11)}$$

Where **m** is the rank of the data and **N** is the total number of elements within the data set.

From this the return period **R** can be derived. The return period is the time taken for an event to be exceeded once on average.

$$R = \frac{1}{1-P} \qquad \text{(Eq.12)}$$

Figs. 13 and 14 are plots of return period versus the peak load on a semi-log axis for both the damped and undamped case. From these graphs a clear relationship between the maximum load and return period can be seen and it is this relationship that makes it possible to carry out an extrapolation on the CDF and predict the loads associated with larger return periods.

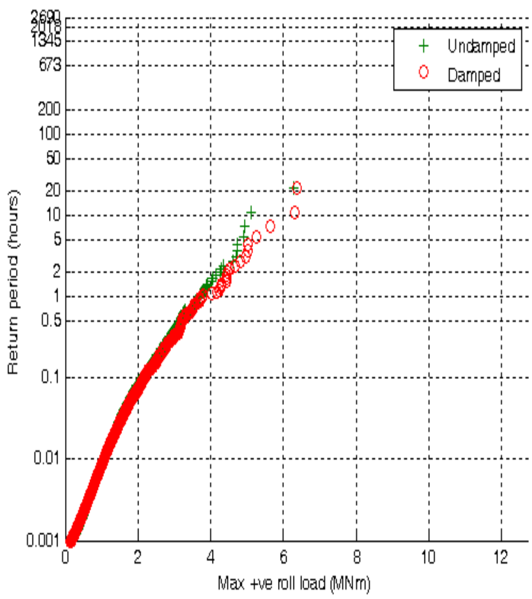

Figure 13: Positive roll extreme value analysis plots for 18m wide, 1.8m thick damped and undamped flap

The extrapolation for larger return periods is complicated somewhat when there is significant deviation from the trend as can be seen in Fig. 13. This scatter of the data points towards the tail of the distribution is associated with the data outliers discussed previously and introduces uncertainty into any loads extrapolated from curves containing such data points.

Fortunately the impact of these data outliers is mitigated by the fact that the loads of greatest concern from a foundation design point of view, heave and surge, are also those in which the loading data generated during tank testing is well conditioned and thus the effect of these outliers is reduced, as shown in Fig. 12.

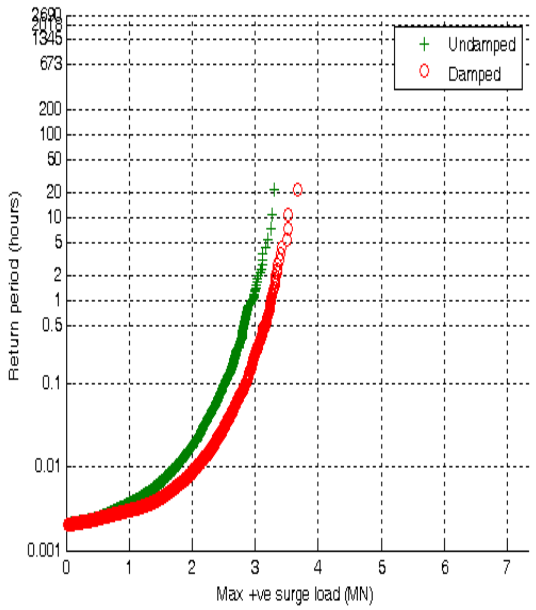

Figure 14: Positive surge extreme value analysis plots for 18m wide, 1.8m thick damped and undamped flap

From Fig. 14 it can be seen that for a globally damped flap the surge foundation load is expected to exceed 4 MN on average approximately once every 400 to 500 hours of extreme sea conditions. Since it is expected that such sea conditions for a period of 26.7 hours per annum and taking the conservative value of 400 hours for the return period, a 4 MN surge load would be expected to be a once in 15 to year event. Using this method it is possible to estimate the expected peak load the device will encounter for a range of different return periods though as you extrapolate for longer return periods it is expected that the error associated with the estimated load will increase.

8. Conclusions and further work

This work presents the design and operating principles behind a novel force transducer used to measure the foundation loads experienced by the Oyster® device under extreme wave loading conditions.

The work has shown that the device is capable of adequately resolving five degrees of freedom so as to provide essential information when tackling the design and implementation of Oyster's foundations.

An outline of the procedures followed while carrying out extreme sea tank testing is given as well as a discussion of the methodology and techniques used during the analysis of the resulting load data.

While work investigating the effect of flap width, thickness, water depth and wave heading angle upon the foundation loads has been carried out the results of these tests has not been presented in this paper.

Further work needs to be carried out to improve the extrapolation methodology used in the extreme value analysis and to investigate the cause of outliers. It is also proposed that proper weighting factors be applied to each extreme sea state to improve the accuracy of the results generated.

Work investigating the effect of different breaking waves upon the device needs to be undertaken using video analysis in parallel with data acquisition to allow a comparison between the measured loads and the wave conditions at the device.

Acknowledgements

The work presented has been funded by Aquamarine Power Ltd and The Engineering and Physical Science Research Council. Support and help from Matt Folley, Max Osterried, David Sloan and Andrew McNulty gratefully acknowledged.

References

[1] M. Folley, T. Whittaker and M. Osterried. The oscillating wave surge converter *Paper No. 2004-JSC-377, 2004*

[2] T. Whittaker, D. Collier, M. Folley, A. Henry and M. Crowley. The development of Oyster-A shallow water surging energy converter *7th European Wave and Tidal Energy Conference, Porto, Portugal, 2007*

[3] N. Berme, P. Lawes, S. Solomonidis and J.P. Paul. A shorter pylon transducer for measurement of prosthetic forces and moments during amputee gait *Engineering in Medicine (I.Mech.E.) 4(4), 6-8, 1976*

[4] N.K. Fowler and A.C Nicol. A force transducer to measure individual finger loads during activities of daily living *Journal of Biomechanics 32(1999) 721-725, 1999*

[5] W. Shi and S.D. Hall. A novel six axis force sensor for measuring the loading of a racing tyre on track *1st International Conference on Sensing technology, Palmerstion North, New Zealand, 2005*

[6] A. Bicchi, A. Caiti and D. Prattichizzo. Dynamic force/torque sensors: Theory and experiments *ICAR'97 Monterey, CA, 1997*

[7] L. Makkonen. Problems in extreme value analysis *Structural Safety 30 405-419, 2008*